Control of a final gating charge transition by a hydrophobic residue in the S2 segment of a K^+ channel voltage sensor

Jérôme J. Lacroix and Francisco Bezanilla[1]

Department of Biochemistry and Molecular Biology, University of Chicago, Gordon Center for Integrative Sciences W244, 929 East 57th Street, Chicago, IL 60637

Contributed by Francisco Bezanilla, March 1, 2011 (sent for review February 1, 2011)

It is now well established that the voltage-sensor domains present in voltage-gated ion channels and some phosphatases operate by transferring several charged residues (gating charges), mainly arginines located in the S4 segment, across the electric field. The conserved phenylalanine F^{290} located in the S2 segment of the Shaker K channel is an aromatic residue thought to interact with all the four gating arginines carried by the S4 segment and control their transfer [Tao X, et al. (2010) *Science* 328:67–73]. In this paper we study the possible interaction of the gating charges with this residue by directly detecting their movement with gating current measurements in 12 F^{290} mutants. Most mutations do not significantly alter the first approximately 80–90% of the gating charge transfer nor the kinetics of the gating currents during activation. The effects of the F^{290} mutants are (*i*) the modification of a final activation transition accounting for approximately 10–20% of the total charge, similar to the effect of the ILT mutant [Ledwell JL, et al. (1999) *J Gen Physiol* 113:389–414] and (*ii*) the modification of the kinetics of the gating charge movement during deactivation. These effects are well correlated with the hydrophobicity of the substituted residue, showing that a hydrophobic residue at position 290 controls the energy barrier of the final gating transition. Our results suggest that F^{290} controls the transfer of R^{371}, the fourth gating charge, during gating while not affecting the movement of the other three gating arginines.

F290 | hydrophobic plug | voltage-dependent gating | sensor-pore coupling

Some membrane proteins possess the ability to detect changes in the electrical potential existent in most cellular membranes. These proteins play crucial roles in generating and propagating nerve impulses along neurons and muscles (1) and also in transducing electrical signals into chemical signals (2, 3). In voltage-sensitive ion channels and some phosphatases, this property is conferred by the voltage-sensor domain (VSD), a canonical protein domain formed by four helices named S1 to S4 (4). The VSD responds steeply to changes in the membrane potential by turning on and off within a few millivolts. This property is conferred by electrical charges, called gating or sensing charges, that feel the electric field across the membrane and drive the VSD into different conformations. The dynamics of the voltage sensor can be studied directly by measurements of the transient currents created by the movements of the gating charges within the electric field (gating currents) (5).

It is now well established that the gating charges consist of conserved electrically charged residues, mostly positive arginines carried by the S4 segment (6, 7) but also negatively charged glutamic and aspartic acids located in the S2 segment (6). Although the precise nature and extent of the conformational rearrangement of the VSD remains debated, it is commonly accepted that VSD activation consists mainly in the relocation of the arginines-rich S4 helix with little movement of the other helices.

In Shaker K channel the first four outermost arginines of the S4 segment change their exposure from the inside at negative membrane potentials to the outside at positive potentials (8, 9). Yet, it is known that the transfer of electrical charges across a cell membrane is quite unfavorable due to the low dielectric environment of the lipid bilayer. How does the voltage sensor circumvent this problem? The crystal structure of Kv channels (10, 11) and molecular dynamics modeling of the structures in membranes (12) show that the gating charges are not exposed to the hydrophobic part of the lipid bilayer. Instead, the gating charges reside in aqueous crevices, and they translocate across a focused electric field (13–17) spanned by a short distance where hydrophobic residues form a hydrophobic plug blocking a "gating pore" (18, 19). The stabilization of the gating charges in either side of this narrow hydrophobic region is thought to be promoted by electrostatic interactions between the positive gating charges and negatively charged residues in other VSD segments, water in the crevices, and also negatively charged phospholipids (20).

F^{290} is a well-conserved aromatic residue located at the bottom of the S2 segment of the Shaker channel (Fig. 1*A*) that faces the intracellular side of the hydrophobic plug (18). In the Kv1.2 structure, the aromatic group of this residue is part of a hydrogen-bonding network with conserved basic residues in S2 and S3 and thus was anticipated to be involved in the gating charge transport (11). Recently, the conductance (G) vs. voltage (V) ($G-V$) relations of F^{290} mutants confirmed the importance of this residue in channel activation. From this study, a gating mechanism where a rigid cyclic side chain at position 290 interacts sequentially with the four gating arginines was proposed (21). However, the nature of the interaction between F^{290} and the gating charges remains unknown. Moreover, in the voltage-gated channel KvAP, which exhibits normal voltage dependence of activation (22), a leucine is present at the position homolog to F^{290} (Fig. 1*A*). Therefore, the validation of this model requires more investigation.

Here we explored the role of this residue by directly measuring the gating currents of 12 F^{290} mutants and analyzed the corresponding charge (Q) vs. voltage (V) ($Q-V$) curve and gating currents kinetics during activation and deactivation. Our results show that the F^{290} mutations do not significantly alter the kinetics nor the voltage dependence of most of the charge movement during activation. These mutations alter the last approximately 10–20% gating transition during activation and dramatically change the deactivation kinetics, showing that, in contrast to its previously proposed role, F^{290} normally controls the energy barrier of only a final gating charge transition. Our data suggest that this transition corresponds to the transfer of R^{371}, the fourth gating arginine. We show that the effects of F^{290} mutants are cor-

Author contributions: J.J.L. and F.B. designed research; J.J.L. performed research; F.B. contributed new reagents/analytic tools; J.J.L. analyzed data; and J.J.L. and F.B. wrote the paper.

The authors declare no conflict of interest.

[1]To whom correspondence should be addressed: E-mail: fbezanilla@uchicago.edu.

This article contains supporting information online at www.pnas.org/lookup/suppl/doi:10.1073/pnas.1103397108/-/DCSupplemental.

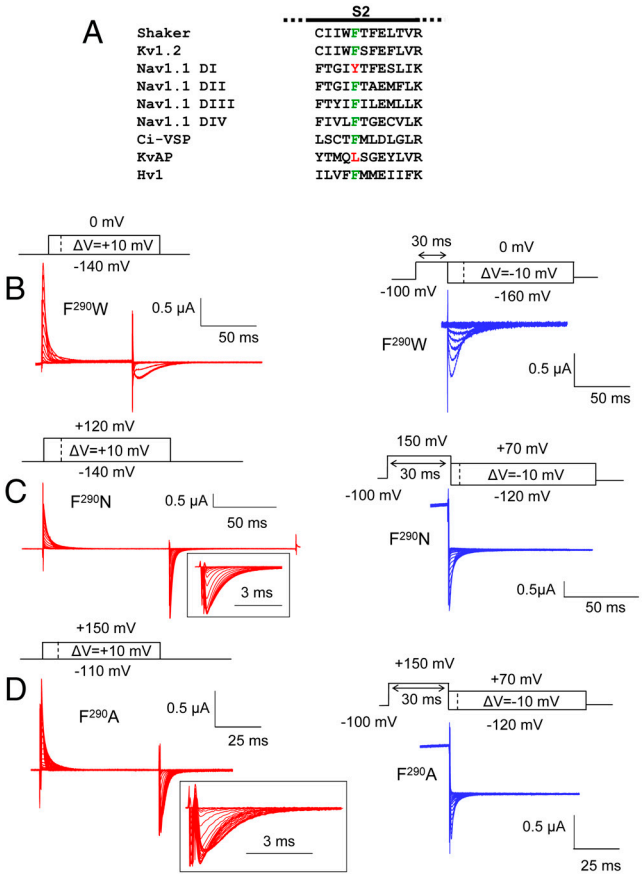

Fig. 1. (*A*) Sequence alignment of the S2 segment of Shaker (GI: 13432103), Kv1.2 (GI: 4826782), Nav1.1 domain I, II, III, and IV (GI: 115583677), Ci-VSP (GI: 76253898), KvAP (GI: 38605092), and Hv1 (GI: 91992155). The residue at position 290 (in Shaker) is colored (green for Phe, red for other amino acid). (*B–D*) Gating currents of the representative mutants $F^{290}W$ (*B*), $F^{290}N$ (*C*), and $F^{290}A$ (*D*) during the indicated activation (red traces) or deactivation (blue traces) protocol. Capacitive and leak currents were subtracted either online using the P/4 method ($F^{290}W$) or using an off-line subtraction ($F^{290}N$ and $F^{290}A$). Gating current traces at the repolarizing pulses of the activation protocol are shown in an expanded time scale for the mutants $F^{290}N$ and $F^{290}A$ (insets).

related with the hydrophobicity of the lateral chain of the substituted residue, inconsistent with a direct interaction of F^{290} with the positive arginines but consistent with a probable role in shaping the electric field inside the voltage sensor.

Results

Voltage Sensing in F^{290} Mutants. We measured the gating currents of 12 F^{290} Shaker mutants (*F* to *W*, *Y*, *I*, *S*, *C*, *M*, *N*, *A*, *G*, *V*, *L*, and *Q*) expressed into *Xenopus* oocytes using the cut-open voltage-clamp technique (23). These mutants were chosen based on their reported high expression (21), a requirement for gating current measurements. Raw gating current traces during activation and deactivation are displayed in Fig. 1 *B–D* for representative mutants. The integration of the gating currents over time determines the amount of charge displaced for each voltage pulse. Typically, the $Q-V$ curve displayed for a voltage-gated channel can be approximately fitted by a two-state Boltzmann function and graphically shows a steep sigmoid relationship. Fig. 2 *A–E* shows the $Q-V$ curves for each tested F^{290} mutant. For most mutants, the charge movement starts at voltages between −80 and −60 mV, similar to wild-type channels that have a Phe in position 290. The only substitution showing a significant change in the initiation of the charge movement is $F^{290}W$, where charge movement occurs at voltages more negative than −100 mV (Fig. 2*A*). The effects of all other F^{290} mutations appear in a late gating transition, at more depolarized potentials. The substitution of F^{290} for *T*, *M*, *N*, and *L*, for instance, produces a shallower turn of the $Q-V$ curve in the positive range (Fig. 2*B*), whereas the substitution for *I*, *G*, *S*, *A*, *Q*, and *V* exhibits $Q-V$ curves with a bisigmoid shape (Fig. 2 *C–E*), isolating a late component of the gating charge movement. In the latter case, the fraction of the total charge contained in this component is not very different among the different mutants and represents approximately 10% to approximately 22%.

To characterize the components revealed by the F^{290} mutations, the $Q-V$ curves of all F^{290} mutants were fitted to a sum of two Boltzmann distributions (see *SI Text*) and an example is shown in Fig. 2*F* for the case of $F^{290}A$. For each mutant, the fit provided the values V_0 and V_1 corresponding, respectively, to the midpoint of the main gating transition and to the midpoint of the minor gating component (Fig. 3*A*). The fitting also gave the apparent valences Z_0 and Z_1 of the main and the minor gating component, respectively (see Table S1), which indicate the steepness of the main and the minor gating component. It is noteworthy that the changes among F^{290} mutants are mostly in the value of V_1 with little variation of V_0 (Fig. 3*A*). Also, the V_1 values correlate well with the midpoint of the conductance (G) vs. voltage curves ($G-V$) reported previously (21). These results indicate that the F^{290} mutants control a late gating component during activation that is associated with pore opening.

If F^{290} were to control the transfer of all the gating charges across the electric field in wild-type Shaker channels as proposed by Tao et al. (21), one would expect that the F^{290} mutations would affect the kinetics of the gating currents. We thus determined the speed of the voltage-sensor movement in F^{290} mutants during activation and also during deactivation, when fully activated channels return to their resting state. Deactivation was studied by prepulsing for 30 ms at a potential strong enough (+100 mV or +150 mV) to move all the gating charges during activation (see *Methods* and Fig. 1 *B–D*) according to the corresponding $Q-V$ curves shown in Fig. 2 *A–E*. The gating currents were fitted with a simple or double exponential function for each test pulse. In the case where a double exponential function was used, a unique time constant was calculated by averaging the two time constants weighted by their relative amplitudes. Fig. 2*F* shows the results for the mutant $F^{290}A$; the results for all the other mutants and wild-type channels are shown in Fig. S1. The maximum values for the time constant during activation (T_A) and deactivation (T_D) (see Fig. 2*F*) were used to compare the speed of activation and deactivation among different mutants. Fig. 3*B* shows that T_D is dramatically affected by the F^{290} mutations, whereas little change in T_A is observed. The most notable kinetic effect on the gating current kinetics during activation is the appearance of a small slow component for some F290 mutants at very positive potentials (Figs. S1 and S2). This slow component corresponds to the transfer of the isolated gating charge.

Fig. 3*C* shows a significant positive correlation ($R=0.83$) between V_1 and the ratio T_A/T_D. For all the F^{290} mutants, as the mutant channel becomes less efficient to open (V_1 higher) the ratio T_A/T_D increases, consistent with the notion that F^{290} controls the energy barrier of the last gating transition that ultimately couples VSD motion to pore opening. We further investigated a possible correlation between the nature of the amino acid inserted at position 290 and its effect on channel gating. Fig. 3*D* shows a significant negative correlation ($R=-0.80$) between V_1 and the hydrophobicity of the side chain of the residue previously determined experimentally (24). These correlations among V_1, T_D, and the hydrophobicity of the substituted residues indicate that a more hydrophobic side chain at the position of F^{290} favors the fully activated state of the VSD (V_1 more negative and T_D larger).

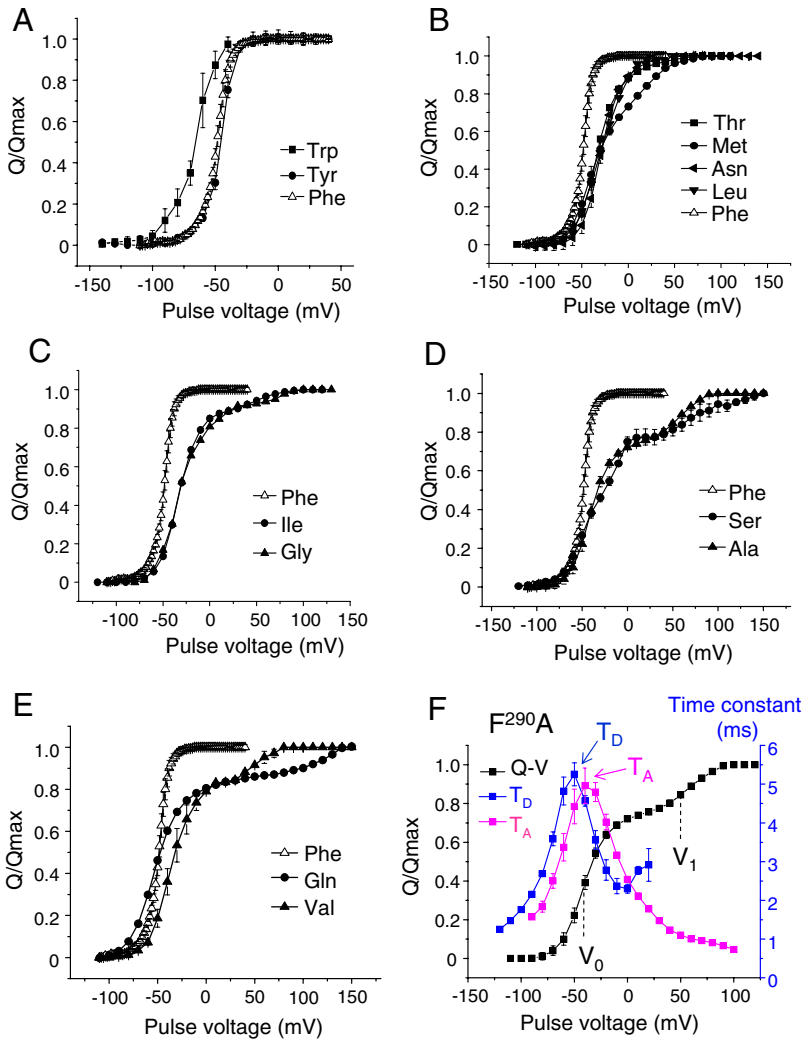

Fig. 2. F^{290} mutations affect a late gating transition of the voltage sensor. (*A–E*) Gating currents were induced by pulsing from a negative voltage (−120 to −140 mV) to incremental more positive voltages and integrated at the repolarizing pulse. The plots show the $Q-V$ curves depending on the residue at position F^{290}. The substituted residues are (*A*) Trp (full squares) and Tyr (full circles); (*B*) Thr (full squares), Met (full circles), Asn (full left triangles), and Leu (full down triangles); (*C*) Ile (full circles) and Gly (full up triangles), (*D*) Ser (full circles) and Ala (full up triangles), and (*E*) Gln (full circles) and Val (full up triangles). In each graph, the $Q-V$ curve of the wild-type F^{290} control is displayed as open up triangles. The data are representative of at least five independent experiments for each mutant. (*F*) Typical gating current analysis depicted for the $F^{290}A$ mutation. The $Q-V$ curve (full squares) was fitted to a sum of two Boltzmann distributions (see *SI Text*), giving the V_0 and V_1 values that are the midpoint values of the two gating charge components. The gating current time constants were measured during activation (magenta squares) and deactivation (blue squares) and plotted as a function of the voltage pulse. The maximum time-constant values are noted T_A and T_D.

The Origin of the Late Gating Charge Component. It is possible to uncouple the voltage-sensor movement and pore opening in Shaker channels by stabilizing a preopen state of the channel with 4-aminopyridine (4-AP) (25, 26) or by introducing three simultaneous mutations at the C terminal of the S4 segment ($V^{369}I$, $I^{372}L$, and $S^{376}T$ (ILT) (27). Pore blocking by 4-AP and the ILT mutations do not prevent most of the voltage-sensor movement, but in either case they isolate a small gating charge transition that represents approximately 10% of the total charge (Fig. 4*A*). This small component is known to correspond to a final transition that appears simultaneously in all four subunits and open the ion permeation pathway in a single step rather than four independent steps (27–29). It is noteworthy that the fraction of the charge contained in this coupling transition is very similar (Fig. 2 *D* and *E*) or nearly undistinguishable to the fraction isolated by the $F^{290}G$ mutant (Fig. 2*C*). Therefore it is reasonable to hypothesize that F^{290} controls the same coupling transition isolated by the ILT mutations or by 4-AP blockade.

We thus studied the effect on gating of combining the ILT and F^{290} mutations. The $Q-V$ and $G-V$ plots of the ILT/$F^{290}T$ double mutant show that the late gating component is shifted to even more positive potentials compared to ILT channels (Fig. 4*B*). In fact, the shift was so large that a full resolution of the $Q-V$ required pulsing the voltage beyond +180 mV, which was not practical. Similarly, it was not possible to determine a voltage value giving the maximal conductance; thus the conductance vs. voltage plots depicted in Fig. 4*B* do not reflect the true $G-V$ curve for this mutant. Nevertheless, these results show that the effects of ILT and the F^{290} mutant are essentially additive.

What is the molecular origin of the charge moving in this coupling transition? In Shaker, the positive gating charges are essentially carried by four arginines residues R^{362} (R1), R^{365} (R2), R^{368} (R3), and R^{371} (R4) distributed along the S4 helix. It is therefore reasonable to hypothesize that the gating component isolated by the F^{290} mutants, which represents 10–22% of the total charge, corresponds to the passage of R4 across the membrane electric field. Interestingly, we found that the isocoulombic mutation R4K produces a split in the $Q-V$ curve, isolating a late component that represents approximately 22% of the total charge (Fig. 4 *C* and *E*). This fraction of the gating charge is identical to the component isolated by the $F^{290}A$ and $F^{290}S$ substitution (Fig. 2*D*). This dramatic effect for a conservative mutation explains the large positive shift of the $G-V$ curve previously observed in R4K channels (30) (also see Fig. 4 *E* and *F*) but absent in R1K, R2K, and R3K channels, the latter exhibiting $Q-V$ and $G-V$ curves very similar to wild-type channels (7, 30).

We further investigated whether the fraction of the charge isolated by the R4K mutation is additive to the one isolated by the $F^{290}T$ mutation. Fig. 4*D* displays gating current recordings for the double mutant R4K/$F^{290}T$ and Fig. 4*F* compares the $Q-V$ and $G-V$ plots of the R4K/$F^{290}T$ and the R4K mutants. In the double mutant, the $G-V$ curve is shifted to negative voltages compared to R4K channels, and its $Q-V$ curve does not display a split but resembles that of the simple mutant $F^{290}T$ (Fig. 2*B*). A similar result is obtained in the double mutant with the $F^{290}A$

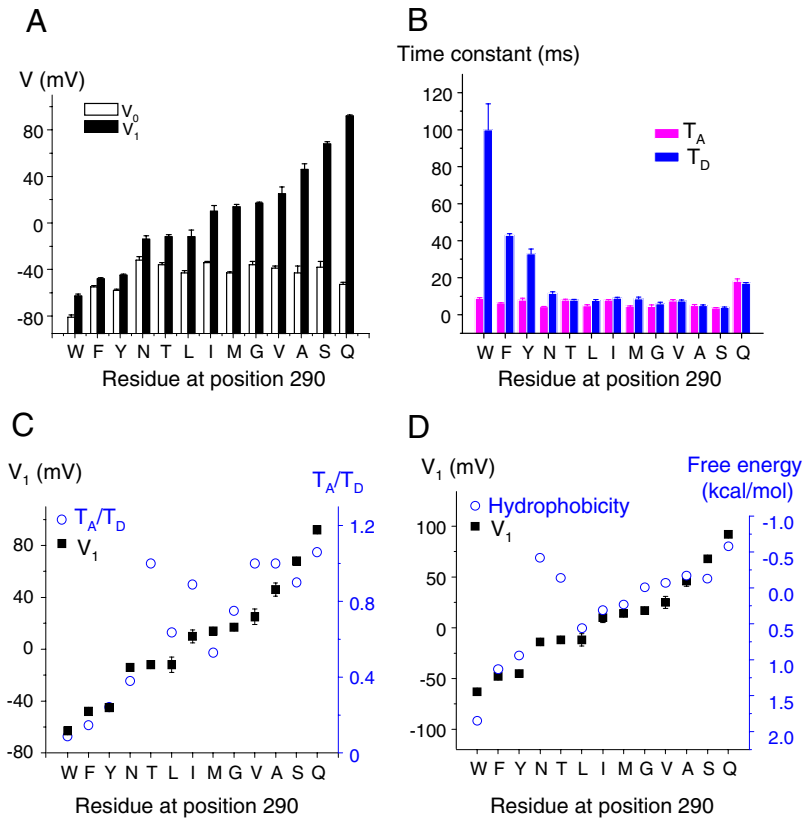

Fig. 3. The effects of the F^{290} mutations depend on the hydrophobicity of the substituted residue. (*A*) Histogram showing the values of V_0 and V_1 for each F^{290} mutant. Note that the mutations affect mainly V_1 with little effect on V_0. (*B*) Histogram showing the values of T_A and T_D for each F^{290} mutant. Note that the mutations affect mainly T_D with little effect on T_A. (*C*) There is a significant correlation ($R \geq 0.80$) between V_1 and the ratio T_A/T_D and (*D*) between V_1 and the hydrophobicity of the residue at position 290. The data are representative of at least five independent experiments for each mutant.

substitution (see Fig. S3). These results thus indicate that the R4K phenotype depends on the residue at position 290, suggesting that F^{290} controls the passage of R4 in wild-type channels.

Discussion

This study aimed at investigating the role of a conserved phenylalanine residue in the S2 segment of the voltage sensor, F^{290}, in Shaker K channels in facilitating the transfer of the S4 arginines during gating. Our results show that F^{290} is not required to transfer most of the gating charge (approximately 80–90%) but rather finely controls a final gating transition representing only approximately 10–20% of the total charge. This is in contrast to the hypothesis put forward by Tao et al. (21) based on a study where the effects of mutations of F^{290} were tested only in the voltage dependence of the conductance. As in the conductance one sees only the last step; one cannot infer unequivocally how every component of the gating charge moves. The authors assumed that F^{290} controls the transfer of all four gating arginines, thus controlling the entire S4 movement. This assumption led to a model that is incompatible with the experimental results presented here. Furthermore, by proposing equivalent gating transitions for all four gating charges, their model also fails to explain the experimentally measured gating shots of $2.4e_0$ during gating that demonstrated that the gating transitions underlying S4 movement during activation do not carry the same amount of charge (31).

In the Tao et al. (21) gating model, more favorable interactions exist between F^{290} and the S4 arginines and between W^{290} and lysines in position 1 or 5 (R1K and K5). Interestingly, the $F^{290}W$ mutant is the only mutation we found to significantly affect the main component of the $Q-V$ curve. The effect of the $F^{290}W$ mutation suggests that a Trp at this position creates an interaction with K5, further stabilizing the activated conformation of the voltage sensor. Because the negative results they obtained for a cation-Π interaction at position 290 were based on benzyl derivatives but not on indole derivatives, it is conceivable that a cation-Π interaction forms between the indole group of Trp^{290} and the positive amino group of K5. This hypothesis is further supported by the fact that a tyrosine or leucine residue can be found besides phenylalanine at the position of 290 in known voltage-sensor sequences (Fig. 1*A*), but not tryptophan. Tryptophan at position 290 was not found in any of the 315 voltage-gated ion-channel-related sequences available in the pfam database (pf00520, http://pfam.sanger.ac.uk/).

We show here that the gating charge component controlled by the residue present at position 290 is similar or in same cases identical to the component isolated by the ILT mutations, 4-AP or the R4K mutation. To us, this suggests that, in each case, the gating perturbation is due to the immobilization of the fourth charge. The small differences in the relative proportion of the isolated component by the different mutations and 4-AP could be explained assuming that the motion of R4 is stopped at slightly different positions relative to the electric field depending on the side chain in position 290, thus isolating a slightly different fraction of the total charge. This hypothesis is largely reinforced by multiple evidences showing that the electric field is strongly focused inside the voltage sensor (8, 9, 13, 15–17, 32–34), forming a hydrophobic plug. Thus, a movement of the positive lateral chain of R4 even a few angstroms within this plug could engender a significant fraction of the channel's gating currents.

The gating charge immobilization by the $F^{290}T$ mutant is additive to the gating charge immobilization by the ILT mutations. These results show that the effects of the ILT and $F^{290}T$ mutations are independent and therefore the ILT residues must be in a different pathway than the $F^{290}T$ mutation during S4 motion. Recently, the gating charge movement in Shaker was shown to strongly depend on the hydrophobicity of the residues intercalated between the S4 charges (35). Because the ILT substitutions ($V^{369}I$, $I^{372}L$, and $S^{376}T$) are located near R3 (R^{368}), R4 (R^{371}), and K5 (K^{375}), it is possible to envisage that the phenotype of the ILT mutant is related to a change in the hydrophobicity in this region. On the other hand, the gating charge immobilization by the $F^{290}T$ or $F^{290}A$ mutation is canceled by the R4K mutation,

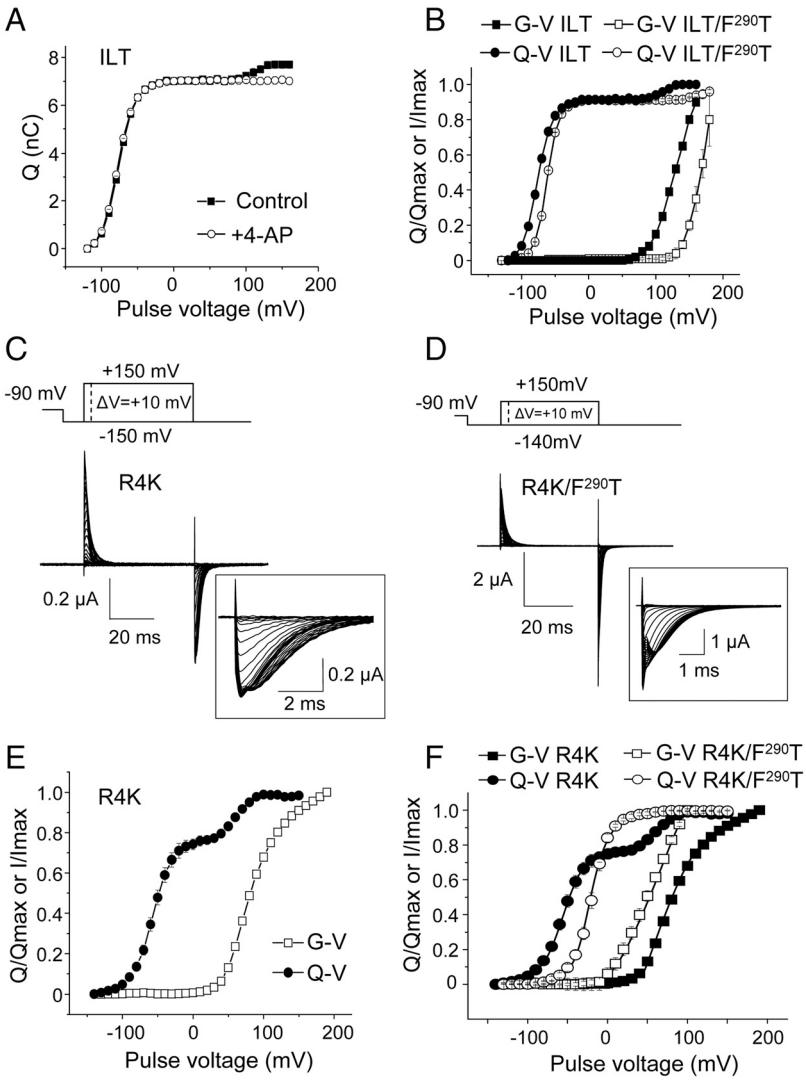

Fig. 4. Two distinct interfaces control the final activation gating transition. (*A*) $Q-V$ curves for the ILT Shaker mutant in the presence (open circles) or absence (full squares) of 1 mM 4-AP. (*B*) $Q-V$ (circles) and $G-V$ (squares) curves of the double mutant ILT/$F^{290}T$ (open symbols) and ILT channels (full symbols). (*C–D*) Gating currents of the R4K mutant (*C*) and the double mutant R4K/$F^{290}T$ (*D*) measured with the indicated activation protocol. The currents' traces at the repolarizing pulses are shown in an expanded time scale (*Insets*). Capacitive and leak currents were subtracted off-line. (*E*) $Q-V$ (full circles) and $G-V$ (open squares) curves for the R4K mutant. (*F*) $Q-V$ (circles) and $G-V$ (squares) curves for the R4K mutation (full symbols) and for the double mutant R4K/$F^{290}T$ (open symbols). The data are representative of four to six independent experiments for each mutant.

suggesting that the lateral chain of the residue present at position 290 is positioned in the same pathway as R4K.

Less hydrophobic residues at position 290 produce faster deactivation kinetics relative to activation, whereas more hydrophobic ones produce slower deactivation kinetics relative to activation. However, the F^{290} mutations have little effects in the activation time constant. These observations indicate that during activation, the main rate limiting transition for the gating charge transfer is the movement of the first (main) fraction of the charge but not the late (minor) fraction, which is the last to cross the electric field. In contrast during deactivation, this minor component is the first to cross the field, and therefore its transfer represents a rate-limiting gating transition. In wild-type Shaker, the deactivation gating currents measured from open channels are normally slowed down compared to activation measured from resting channels (36). This phenomenon was recently shown to involve intersubunit interactions between the C-terminal portion of the S4 and the S6 segment (37), which are created concomitantly to pore opening. Here, we show that the F^{290} mutations that produce the strongest immobilization of the late gating transition also produce the fastest deactivation gating kinetics. This observation supports our hypothesis that F^{290} controls the energy barrier of the final gating charge transition during activation, which becomes the initial gating transition during deactivation.

Several lines of evidences support the notion that the S4 segment adopts a 3_{10} conformation during the gating charges transfer (11, 12, 38, 39). A direct consequence of the S4 moving as a 3_{10} helix is that the lateral chains of the arginines are lined up along one face of the S4. However, in our interpretation, Phe290 controls the transfer of R4, suggesting that the latter is not moving in the same pathway as R1–R3. This seems paradoxical if one considers the 3_{10} helix hypothesis where R1–R4 point in the same direction. However, this paradox exists solely if the S4 helix moves linearly as a rigid body without rotation/tilt and in the direction of its own axis during gating. Although the exact motion of S4 is still debated, there is evidence that the S4 movement has several spatial components (tilt and rotation) during its vertical ascension. Therefore our interpretation that R4 is not moving in the same pathway as R1–R3 does not exclude a S4 movement in a 3_{10} helix conformation.

The gating charge immobilization by F^{290} mutants depends on the hydrophobicity of the substituted residue such that the transfer of the last charge is easier when a more hydrophobic side chain is present. This observation does not support a direct interaction of a hydrophobic residue present at position 290 with the positively charged arginines. The negative results of a possible cation-Π interaction mediated by F^{290} (21) is another evidence against a direct interaction. In a refined native structure of Kv1.2, F^{290} is located at the lower end of the hydrophobic plug (18). Therefore, we propose that a hydrophobic residue at the position of F^{290} defines the intracellular boundary for the hydrophobic plug and that this function is better fulfilled with more hydrophobic lateral chains, which help in maintaining a low dielectric barrier.

In summary, our study singles out the hydrophobicity of the residue present at position F^{290} in Shaker K channels as a critical molecular determinant that controls the final gating transition of the voltage sensor that normally produces channel opening and also helps in stabilizing the open state of the pore.

Methods

Mutagenesis and Expression in *Xenopus* oocytes. All mutations were introduced by PCR using degenerated primers (Quick Change, Stratagene) from a pBSTA plasmid encoding the N-type inactivation removed (Δ6-46) version of the Shaker K^+ channel and modified as previously described (8). For gating current measurements, the cDNA contained the additional W434F mutation that prevents ion conduction (40). Positive clones were identified by sequencing the entire Shaker cDNA. Mutated cDNAs were linearized with a unique Not1 restriction site (enzyme purchased from New England Biolabs) and transcribed into cRNAs using a T7 RNA expression kit (Ambion). Thirty to 50 ng of cRNA were injected into *Xenopus* oocytes usually 24 h after their surgical extraction from adult frogs. Injected oocytes were maintained before recordings in a standard oocytes solution containing 100 mM NaCl, 5 mM KCl, 2 mM $CaCl_2$, and 10 mM Hepes at pH 7.5 for 2 to 6 d at 16.5 °C.

Electrophysiological Recordings and Data Analyses. Electrophysiology experiments were made using the cut-open voltage-clamp method (23). For gating current recordings, the internal solution was 115 mM N-methyl-D-glucamine (NMG) methanesulfonate (MES), 2 mM EGTA, and 10 mM Hepes pH 7.5; the external solution contained 115 mM NMG-MES, 2 mM Ca-MES, and 10 mM Hepes pH 7.5. For 4-AP experiments, 1 mM of 4-AP was added in the external solution while the holding potential was raised to 0 mV for 2 min. Typical holding potentials were −80 or −90 mV. Activation gating was induced by prepulsing for 60 ms to −120 mV or −140 mV prior a test pulse of +10 mV increment to more positive potentials. Deactivation gating was induced by prepulsing for 30 ms to +0 mV (wild-type Shaker, $F^{290}Y$ and $F^{290}W$), +100 mV ($F^{290}T$, $F^{290}M$, $F^{290}A$, and $F^{290}L$), or +150 mV ($F^{290}Q$, $F^{290}V$, $F^{290}I$, $F^{290}G$, $F^{290}S$, and $F^{290}A$). For ionic current recordings, the external solution contained 11.5 mM K-MES, 103.5 mM NMG-MES, 2 mM Ca-MES, and 10 mM Hepes pH 7.5 and the internal solution contained 115 mM K-MES, 2 mM EGTA, and 10 mM Hepes pH 7.5. The recording pipette resistance was 0.8 to 1.5 MΩ. Data were acquired at a sampling frequency from 30 to 100 kHz and filtered online at 5 to 20 kHz using a low pass Bessel filter mounted in the amplifier (Dagan). For gating current recordings, capacitive transient currents were subtracted online using the P/4 method when possible. Data were stored and analyzed using in-house software.

ACKNOWLEDGMENTS. This work was supported by National Institutes of Health Grant GM030376.

1. Hodgkin AL, Huxley AF (1952) A quantitative description of membrane current and its application to conduction and excitation in nerve. *J Physiol* 117:500–544.
2. Murata Y, et al. (2005) Phosphoinositide phosphatase activity coupled to an intrinsic voltage sensor. *Nature* 435:1239–1243.
3. Ben-Chaim Y, et al. (2006) Movement of 'gating charge' is coupled to ligand binding in a G-protein-coupled receptor. *Nature* 444:106–109.
4. Kubo Y, Baldwin TJ, Jan YN, Jan LY (1993) Primary structure and functional expression of a mouse inward rectifier potassium channel. *Nature* 362:127–133.
5. Armstrong CM, Bezanilla F (1973) Currents related to movement of the gating particles of the sodium channels. *Nature* 242:459–461.
6. Seoh SA, Sigg D, Papazian DM, Bezanilla F (1996) Voltage-sensing residues in the S2 and S4 segments of the Shaker K+ channel. *Neuron* 16:1159–1167.
7. Aggarwal SK, MacKinnon R (1996) Contribution of the S4 segment to gating charge in the Shaker K+ channel. *Neuron* 16:1169–1177.
8. Starace DM, Bezanilla F (2001) Histidine scanning mutagenesis of basic residues of the S4 segment of the shaker k+ channel. *J Gen Physiol* 117:469–490.
9. Larsson HP, Baker OS, Dhillon DS, Isacoff EY (1996) Transmembrane movement of the shaker K+ channel S4. *Neuron* 16:387–397.
10. Long SB, Campbell EB, Mackinnon R (2005) Crystal structure of a mammalian voltage-dependent Shaker family K+ channel. *Science* 309:897–903.
11. Long SB, Tao X, Campbell EB, MacKinnon R (2007) Atomic structure of a voltage-dependent K+ channel in a lipid membrane-like environment. *Nature* 450:376–382.
12. Khalili-Araghi F, et al. (2010) Calculation of the gating charge for the Kv1.2 voltage-activated potassium channel. *Biophys J* 98:2189–2198.
13. Asamoah OK, Wuskell JP, Loew LM, Bezanilla F (2003) A fluorometric approach to local electric field measurements in a voltage-gated ion channel. *Neuron* 37:85–97.
14. Starace DM, Stefani E, Bezanilla F (1997) Voltage-dependent proton transport by the voltage sensor of the Shaker K+ channel. *Neuron* 19:1319–1327.
15. Islas LD, Sigworth FJ (2001) Electrostatics and the gating pore of Shaker potassium channels. *J Gen Physiol* 117:69–89.
16. Ahern CA, Horn R (2005) Focused electric field across the voltage sensor of potassium channels. *Neuron* 48:25–29.
17. Starace DM, Bezanilla F (2004) A proton pore in a potassium channel voltage sensor reveals a focused electric field. *Nature* 427:548–553.
18. Chen X, Wang Q, Ni F, Ma J (2010) Structure of the full-length Shaker potassium channel Kv1.2 by normal-mode-based X-ray crystallographic refinement. *Proc Natl Acad Sci USA* 107:11352–11357.
19. Campos FV, Chanda B, Roux B, Bezanilla F (2007) Two atomic constraints unambiguously position the S4 segment relative to S1 and S2 segments in the closed stateof Shaker K channel. *Proc Natl Acad Sci USA* 104:7904–7909.
20. Schmidt D, Jiang QX, MacKinnon R (2006) Phospholipids and the origin of cationic gating charges in voltage sensors. *Nature* 444:775–779.
21. Tao X, et al. (2010) A gating charge transfer center in voltage sensors. *Science* 328:67–73.
22. Schmidt D, Cross SR, MacKinnon R (2009) A gating model for the archeal voltage-dependent K(+) channel KvAP in DPhPC and POPE:POPG decane lipid bilayers. *J Mol Biol* 390:902–912.
23. Stefani E, Bezanilla F (1998) Cut-open oocyte voltage-clamp technique. *Methods Enzymol* 293:300–318.
24. Wimley WC, White SH (1996) Experimentally determined hydrophobicity scale for proteins at membrane interfaces. *Nat Struct Biol* 3:842–848.
25. Loboda A, Armstrong CM (2001) Resolving the gating charge movement associated with late transitions in K channel activation. *Biophys J* 81:905–916.
26. Armstrong CM, Loboda A (2001) A model for 4-aminopyridine action on K channels: similarities to tetraethylammonium ion action. *Biophys J* 81:895–904.
27. Smith-Maxwell CJ, Ledwell JL, Aldrich RW (1998) Uncharged S4 residues and cooperativity in voltage-dependent potassium channel activation. *J Gen Physiol* 111:421–439.
28. Ledwell JL, Aldrich RW (1999) Mutations in the S4 region isolate the final voltage-dependent cooperative step in potassium channel activation. *J Gen Physiol* 113:389–414.
29. Gagnon DG, Bezanilla F (2010) The contribution of individual subunits to the coupling of the voltage sensor to pore openingin Shaker K channels: effect of ILT mutations in heterotetramers. *J Gen Physiol* 136:555–568.
30. Papazian DM, Timpe LC, Jan YN, Jan LY (1991) Alteration of voltage-dependence of Shaker potassium channel by mutations in the S4 sequence. *Nature* 349:305–310.
31. Sigg D, Stefani E, Bezanilla F (1994) Gating current noise produced by elementary transitions in Shaker potassium channels. *Science* 264:578–582.
32. Yang N, Horn R (1995) Evidence for voltage-dependent S4 movement in sodium channels. *Neuron* 15:213–218.
33. Yang N, George AL, Jr, Horn R (1996) Molecular basis of charge movement in voltage-gated sodium channels. *Neuron* 16:113–122.
34. Tombola F, Pathak MM, Isacoff EY (2005) Voltage-sensing arginines in a potassium channel permeate and occlude cation-selective pores. *Neuron* 45:379–388.
35. Xu Y, Ramu Y, Lu Z (2010) A shaker K+ channel with a miniature engineered voltage sensor. *Cell* 142:580–589.
36. Bezanilla F, Perozo E, Stefani E (1994) Gating of Shaker K+ channels: II. The components of gating currents and a model of channel activation. *Biophys J* 66:1011–1021.
37. Batulan Z, Haddad GA, Blunck R (2010) An intersubunit interaction between S4-S5 linker and S6 is responsible for the slow off-gating component in Shaker K+ channels. *J Biol Chem* 285:14005–14019.
38. Villalba-Galea CA, Sandtner W, Starace DM, Bezanilla F (2008) S4-based voltage sensors have three major conformations. *Proc Natl Acad Sci USA* 105:17600–17607.
39. Bjelkmar P, Niemela PS, Vattulainen I, Lindahl E (2009) Conformational changes and slow dynamics through microsecond polarized atomistic molecular simulation of an integral Kv1.2 ion channel. *PLoS Comput Biol* 5:e1000289.
40. Perozo E, MacKinnon R, Bezanilla F, Stefani E (1993) Gating currents from a nonconducting mutant reveal open-closed conformations in Shaker K+ channels. *Neuron* 11:353–358.